Capillarity

Vol. 17, No. 1, p. 16-26, 2025

Original article

Pore-scale investigation of the effects of wetting phase re-imbibition on gas capillary trapping in porous media

Chunwei Zhang[1,2], Kai Zhang[1,2], Sota Yoshida[3], Zijing Li[3,4]*, Wei Zhao[5], Tetsuya Suekane[3]

[1]*National Key Laboratory of Automotive Chassis Integration and Biomimetics, Jilin University, Changchun 130025, P. R. China*

[2]*College of Automotive Engineering, Jilin University, Changchun 130025, P. R. China*

[3]*Department of Mechanical Engineering, Institute of Science Tokyo, Tokyo 152-8550, Japan*

[4]*Institutes of Innovation for Future Society, Nagoya University, Nagoya 464-8601, Japan*

[5]*State Key Laboratory of Petroleum Resources and Engineering, China University of Petroleum, Beijing 102249, P. R. China*

Keywords:
Capillary trapping
re-imbibition
injection direction
capillary number

Cited as:
Zhang, C., Zhang, K., Yoshida, S., Li, Z., Zhao, W., Suekane, T. Pore-scale investigation of the effects of wetting phase re-imbibition on gas capillary trapping in porous media. Capillarity, 2025, 17(1): 16-26.
https://doi.org/10.46690/capi.2025.10.02

Abstract:
Capillary trapping of the non-wetting phase in porous media is vital for long-term CO_2 sequestration and underground gas storage. While injection strategies have received extensive research attention, the pore-scale mechanisms controlling residual gas stability during wetting phase re-imbibition under varying injection directions coupled with buoyancy remain unclear. This study used high-resolution micro-focus X-ray computed microtomography imaging and quantitative analysis to investigate gas trapping in a hydrophilic glass bead pack across multiple capillary numbers. Both downward (gravity-aligned) and upward (gravity-opposing) re-imbibition were tested. The results demonstrate that downward injection promotes bubble fragmentation and stabilization, sustaining higher residual saturation, increased populations of small bubbles, and greater specific surface area even under elevated capillary numbers. Upward injection, in which buoyancy aligns with flow, enhances bubble coalescence and mobilization, lowering residual saturation and trapping efficiency. These pore-scale trends highlight the critical interplay of capillary, viscous, and buoyancy forces in shaping gas trapping behavior. The findings of this study provide valuable experimental insights for optimizing injection direction and flow rate, in order to improve long-term CO_2 storage security and underground gas storage operations.

1. Introduction

Capillary trapping of the non-wetting phase is a crucial and widespread physical mechanism in porous media (Scanziani et al., 2020), which underpins the stability of natural systems and the reliable operation of various engineering applications. Examples include controlling the migration of non-aqueous phase organic contaminants, Carbon Capture and Storage, and Underground Gas or Hydrogen Storage systems (Hassanpouryouzband et al., 2021; Zhang et al., 2021a; Padhye et al., 2023). By restricting the continuous migration of fluids, capillary trapping improves storage efficiency and enhances the long-term stability of the system (Chen et al., 2025a). Capillary trapping, along with structural, solubility and mineral trapping, constitutes a multi-tiered CO_2 storage mechanism in the subsurface in carbon capture and storage scenarios (Alcalde et al., 2018). Specifically, capillary trapping not only aids in establishing an early-stage containment barrier but also serves as a cushion gas at the reservoir base, thereby increasing the

Yandy Scientific Press

*Corresponding author.
E-mail address: zcw611985@jlu.edu.cn (C. Zhang); zhangkai23@mails.jlu.edu.cn (K. Zhang); yoshida.s.az@m.titech.ac.jp (S. Yoshida); li.zijing.x0@f.mail.nagoya-u.ac.jp (Z. Li); zhaowei_cup2023@163.com (W. Zhao).

Received June 19, 2025; revised July 15, 2025; accepted August 1, 2025; available online August 4, 2025.

resistance of the system to buoyancy and enhancing long-term storage security (He et al., 2024). Compared to other relatively slow chemical trapping processes (Chen et al., 2024), such as solubility trapping and mineral trapping, capillary trapping responds more rapidly and provides more stable containment (Thaysen et al., 2023). This stability is largely attributed to the mechanism inherent to capillary trapping (Cai et al., 2021), which is governed by pore-scale gas-liquid interfacial tension, the geometric confinement of gas bubbles, and the wettability of the porous medium (Hu et al., 2021; Patmonoaji et al., 2023; Wang et al., 2023). As a result, capillary trapping exhibits relatively low sensitivity to macroscopic geological disturbances (Krevor et al., 2015). Despite its proven effectiveness at the field scale, the pore-scale mechanisms governing capillary trapping under different injection modes remain insufficiently understood. In particular, the effects of wetting phase re-imbibition on the spatial stability, connectivity and interfacial morphology of trapped gas have yet to be systematically verified at the pore scale (Krevor et al., 2015), and the interpretation of the underlying mechanisms remain incomplete.

Recent studies have demonstrated that injection strategies play a crucial role in regulating capillary trapping of the non-wetting phase and can trigger a series of noteworthy multiphase interfacial phenomena (Zhou et al., 2024). Specifically, variations in injection rate significantly affect trapping efficiency, primarily due to the competition between capillary and viscous forces (Lenormand et al., 1988). At low injection rates, capillary forces dominate, stabilizing gas-liquid interfaces and immobilizing bubbles in pore spaces. Conversely, higher injection rates strengthen viscous forces. This phenomenon tends to distort or displace gas interfaces, enhancing bubble mobilization and reducing the likelihood of trapping (Mo et al., 2024). This dynamic competition governs the extent of residual gas retention during re-imbibition. According to displacement phase diagrams (Hu et al., 2020a), different combinations of capillary number and viscosity ratio determine the prevailing displacement mode, such as capillary fingering, viscous fingering, or stable displacement, which in turn dictate the evolution of gas-liquid interfaces and the spatial distribution of the residual phase. Spurin et al. (2024) highlighted that a "fast-then-slow" injection strategy is more favorable for stabilizing trapped structures than constant-rate injection and it shows lower sensitivity to pore-scale heterogeneity. In addition, changes in the injection direction can substantially alter the interfacial evolution pathways and the amount of trapped gas during a single displacement event (He et al., 2023). This arises from inlet pore-throat connectivity and structural anisotropy (Maggiolo et al., 2021). Meanwhile, the flow direction determines whether the capillary pressure gradient aligns with buoyancy, making this mechanism especially important in systems with significant gravitational effects (Li et al., 2024). In addition to conventional injection strategies, various enhanced methods have been proposed to further improve capillary trapping. For instance, the huff-n-puff technique has been widely applied in unconventional oil and gas recovery and CO_2 sequestration (Chen et al., 2025b), where alternating cycles of injection, shut-in and production stages promote the spatial rearrangement of gas within the pore network (Wang et al., 2025b). Na et al. (2011) proposed a co-injection strategy in which CO_2 and water are injected simultaneously to optimize the initial gas distribution, followed by subsequent water flooding to enhance *in-situ* capillary trapping. Similarly, Herring et al. (2016) demonstrated that cyclic injection can enhance supercritical CO_2 trapping by promoting the formation of preferential flow pathways. These pathways may induce a memory effect (Holtzman et al., 2020), which guides subsequent fluid migration along established paths and further stabilizes CO_2 trapping, dissolution, and local solute dispersion (Wang et al., 2023; Saeibehrouzi et al., 2025; Xue et al., 2025; Zhang et al., 2025). Despite the above advances in understanding the effects of injection rates, operational strategies, and various injection modes on capillary trapping, the role of injection direction during wetting phase re-imbibition following gas injection remains systematically understudied. In particular, the coupling between injection direction and gravity, as well as its buoyancy-driven effects on bubble connectivity, interfacial stability, and pore-scale trapping morphology, requires further elucidation.

Wetting phase re-imbibition commonly occurs during late-stage CO_2 sequestration (Qin et al., 2025), water table fluctuations, or injection scheme adjustments, and significantly impacts non-wetting phase trapping behavior (Krevor et al., 2015). Compared to primary drainage, the interfacial dynamics during re-imbibition are more complex and often involve bubble rearrangement, snap-off, morphological reconstruction, or even local detachment. Berg et al. (2013) performed X-ray computed microtomography (X-ray CT) experiments to demonstrate that in hydrophilic porous media, wetting phase re-imbibition readily induces gas-liquid interface snap-off (Zhang et al., 2021c), and that the formation of trapped gas bubbles strongly depends on pore throat geometry and wettability conditions, especially under capillary-dominated flow regimes. Using a series of micro-CT experiments, Hu et al. (2020b, 2021) investigated the effects of capillary number and wettability on non-wetting phase trapping and interfacial structure. They found that at low capillary numbers, bubble volume distributions exhibit power-law characteristics and the residual saturations remain relatively stable, whereas at high capillary numbers, bubbles tend to break up and form isolated structures. Different wettability conditions also alter the spatial distribution of bubbles and interfacial contact area, thereby regulating mass transfer processes. The above studies indicate that injection rate and wettability jointly control trapping morphology and interfacial stability, which are key factors influencing mass exchange efficiency. Wang et al. (2025a) further pointed out that during CO_2 re-injection, interfacial evolution directly affects capillary trapping and gas dissolution efficiency, with wettability and injection rate acting as major controlling factors. Existing research has mainly focused on flow patterns where two-phase fluids are injected in the same direction, particularly in cyclic injection scenarios where injection and production stages typically follow a fixed flow direction (Wang et al., 2023; Saeibehrouzi et al., 2025; Yang et al., 2025). However, studies on counter-injection, where the wetting phase is re-injected opposite to the original flow

direction of the non-wetting phase, remain relatively scarce. Bagheri et al. (2023) used pore-scale simulations to model a drainage and re-imbibition sequence with counter-directional injection and extraction, demonstrating how capillary number and gas compressibility affect storage efficiency. However, their simulation did not explicitly consider gravitational forces or buoyancy effects, which are in fact crucial for understanding how flow direction interacts with capillary pressure gradients in real geological settings. In particular, because of the absence of a gravity field in their model, the potential stabilizing or destabilizing effects of buoyancy-driven flow on trapped structures are still unclear. In a similar fashion, Lysyy et al. (2022) conducted microfluidic experiments to simulate hydrogen storage in aquifers and showed that multiple displacement mechanisms and non-equilibrium gas dissolution can occur during re-imbibition. While their study highlighted the complexity of pore-scale re-imbibition dynamics, it maintained a fixed injection pathway, leaving open the question of how variations in injection direction, especially when coupled with gravity, may influence capillary trapping morphology and residual gas connectivity. The above studies indicate that, despite advances in numerical modeling and microfluidic visualization, the combined effect of injection direction and buoyancy during wetting phase re-imbibition still lacks systematic pore-scale experimental evidence and a mechanistic understanding.

In summary, although previous research has investigated multiphase displacement mechanisms and the effects of injection strategies on capillary trapping in considerable depth, the behavior of gas trapping during wetting phase re-imbibition under the coupled influence of varying injection directions and buoyancy remains insufficiently explored. In particular, the pore-scale evolution of trapped structures, bubble morphology reconstruction, and re-mobilization mechanisms still lack systematic experimental validation and a mechanistic interpretation. This is especially valid for underground gas storage and enhanced oil recovery applications, where buoyancy and capillary forces in vertical flows interact strongly and significantly influence residual gas behavior. Studying vertical rather than horizontal displacement processes is essential because buoyancy acts primarily in the vertical direction and significantly interacts with the flow during re-imbibition (Li et al., 2024). In upward injection, buoyancy aligns with the wetting-phase flow, promoting gas bubble mobilization and coalescence. In contrast, during downward injection, buoyancy opposes the flow, stabilizing residual gas by inhibiting upward migration. These directional interactions between buoyancy and capillary forces directly influence the morphology, stability and spatial distribution of trapped gas. In horizontal displacement, buoyancy has little or no impact, making vertical flows more critical in understanding gas trapping behavior in subsurface environments. Therefore, using a hydrophilic glass bead porous medium as a model system, this study combines high-resolution X-ray CT scanning with image reconstruction analysis to systematically investigate gas capillary trapping behavior under different injection directions (aligned with and opposite to gravity), multiple re-imbibition cycles, and multi-stage flow rates characterized by the capillary number. By quantitatively analyzing residual gas saturation, bubble volume distributions, specific surface area, and re-aggregation characteristics, it is elucidated how the coupling between injection direction and buoyancy affects the stability and morphological evolution of capillary trapping, aiming to provide pore-scale physical insights and practical references for optimizing injection strategies in CO_2 geological storage and other porous media storage applications.

2. Methods and materials

2.1 Experimental apparatus and materials

A transparent cylindrical acrylic column with an inner diameter of 11.0 mm and a height of 21 mm was used as the experimental vessel to construct the packed model porous medium (Li et al., 2023), as shown in Fig. 1(a). The column was uniformly packed with hydrophilic glass beads (average diameter approximately 400 μm) and vibrated to achieve a dense, unconsolidated structure. To enhance the identification of gas-liquid-solid phase interfaces during X-ray imaging, the wetting phase was prepared by dissolving 15 wt% sodium iodide (NaI) in deionized water (Zhang et al., 2021b), while air served as the non-wetting phase. The entire system was installed in a micro-focus X-ray CT scanner (ScanXmate-CF110TSS300, Comscantechno Co., Japan) with an image resolution of 992×992 pixels, a spatial resolution of approximately 17.2 μm per pixel, and a scanning frequency of 4 frames per second. The detailed CT settings and operating procedures can be found in our previous work (Hu et al., 2020a, 2020b). To ensure stable and adjustable flow rates, the injection of the wetting phase was controlled by a programmable syringe pump (kdScientific KDS-210). All experiments were conducted at room temperature (approximately 293 K) and atmospheric pressure (0.1 MPa). The measured parameters, including liquid viscosity, water-gas density difference, and interfacial tension, were used to calculate the capillary number ($Ca = \mu u/\sigma$), which represents the ratio of viscous to capillary forces, and the Bond number ($Bo = \Delta\rho g d^2/\sigma$), which describes the relative importance of buoyancy compared to capillary forces. Here, μ represents the dynamic viscosity, u represents the injection velocity, σ represents the interfacial tension, $\Delta\rho$ represents the density difference between water and gas, g represents the gravitational acceleration, and d is the characteristic length (mean bead diameter). For the experimental conditions set in this study, assuming $\mu = 10^{-3}$ Pa·s, $\Delta\rho$ = 1,000 kg/m^3, $g = 9.81$ m/s^2, $\sigma = 0.07$ N/m, and $d = 400$ μm, the Bond number is approximately 0.0225. Notably, while the capillary number varies with injection velocity, the Bond number remains constant, reflecting the fixed ratio of buoyancy to capillary forces in the porous medium.

2.2 Experimental procedures

The experimental procedure, illustrated in Fig. 1(a), began with densely packing hydrophilic glass beads (average diameter approximately 400 μm) into the transparent acrylic column, which was vibrated to achieve a dense (Hu et al., 2020b), unconsolidated structure and then physically sealed. The packed column was fully saturated with the wetting phase (15 wt% NaI solution) by vacuum degassing, which removes trapped air

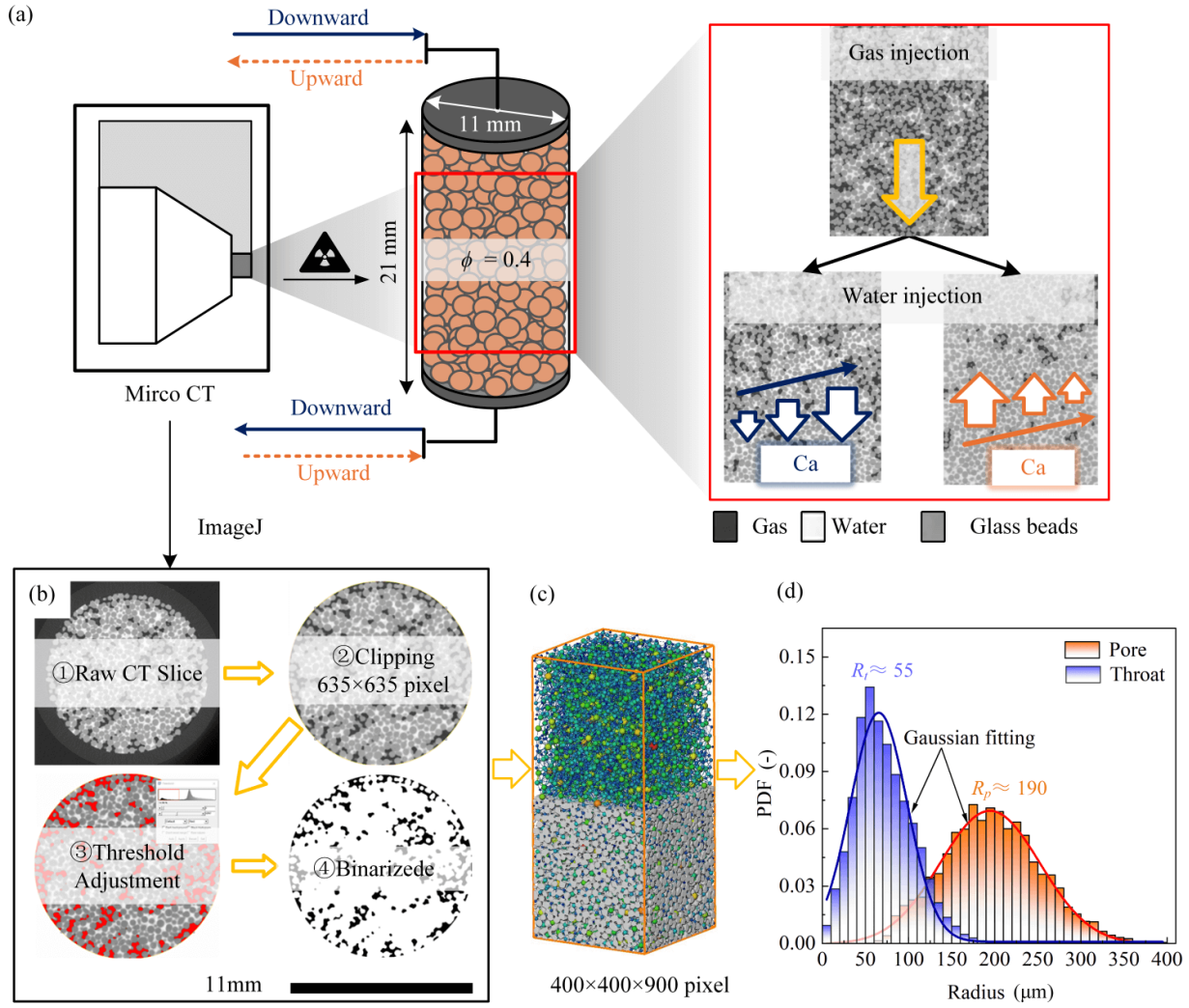

Fig. 1. (a) Schematic of the experimental procedure with gas injection and wetting phase re-imbibition under upward and downward conditions at varying capillary numbers, (b) CT image processing steps: Raw slice, clipping, thresholding, and binarization, (c) the reconstructed pore network model for quantitative analysis, and (d) pore and throat size distribution with Gaussian fitting.

and allows capillary forces to draw the solution into the pore spaces as the pressure gradually returns to atmospheric conditions. Full saturation was confirmed by X-ray CT scanning, after which air was injected from the top at a flow rate corresponding to a capillary number of $\log Ca = -4.24$, displacing part of the liquid downward to establish a stable residual gas structure as the initial condition for subsequent tests. Subsequently, the wetting phase was re-injected at controlled flow rates, corresponding to capillary numbers ($\log Ca$) ranging from approximately -5.1 to -4.1, reflecting increasing injection intensity. Re-injection was performed in two directions: Downward (gravity-aligned) and upward (gravity-opposing). For each capillary number and injection direction, approximately 10 Pore Volumes (PV) were injected per cycle, with each pore volume corresponding to roughly 0.8 mL. After each injection, an immediate CT scan was performed to capture the residual gas distribution, and this injection-scan sequence was repeated three times to visualize the pore-scale evolution of trapped gas morphology. Once re-imbibition was completed at a specific flow rate, the syringe pump was adjusted to a different flow rate to achieve a new capillary number, and the same process was repeated to compare structural responses under varying displacement intensities.

2.3 Image processing

The image processing workflow is illustrated in Fig. 1(b). ImageJ software was used for all image processing tasks, including three-dimensional (3D) reconstruction and quantitative analysis. Initially, a central region of 635×635 pixels was extracted from each CT slice, totaling 910 slices to form a cylindrical volume with a diameter of 10.9 mm and a height of 15.67 mm. Non-local means filtering was applied to enhance phase contrast, followed by preliminary segmentation using Otsu's thresholding method to extract pore boundaries (Li et

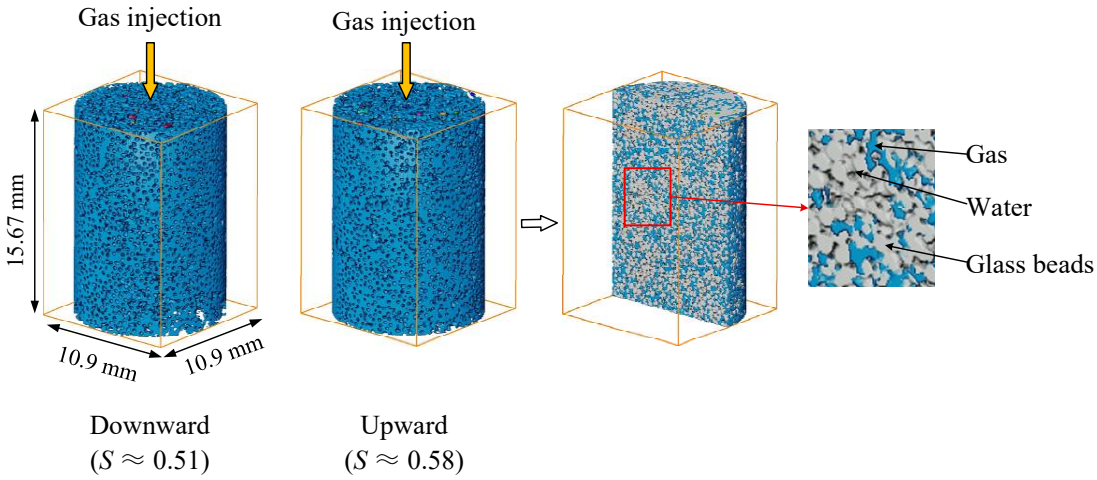

Fig. 2. Initial gas distributions established by downward gas injection, used as the initial condition for downward and upward re-imbibition. Blue, transparent and gray represent gas, water and glass beads, respectively.

al., 2023). Geometric registration was performed by fitting the central positions and edge trends of each slice in horizontal and vertical directions to correct sample tilt and displacement during scanning. After registration, the porous region was cropped and median filtering was applied to remove background noise. Subsequently, segmented thresholding was used to isolate the gas phase, and quantitative parameters such as bubble volume, count, and specific surface area were calculated using the 3D Object Counter and MorphoLibJ plugins. Bubbles with fewer than 50 voxels were excluded to ensure statistical reliability (Hu et al., 2021). The reconstructed pore network model and pore-throat extraction results are shown in Fig. 1(c), where the characteristic pore and pore-throat diameter is approximately 190 and 55 μm, respectively. The probability density distribution of pore throat sizes, fitted by a Gaussian function, is presented in Fig. 1(d). These characterizations provide fundamental data for subsequent multiphase flow and trapping structure analyses.

The initial trapped gas configurations were established following primary gas injection from the top of the column in a downward direction. This process displaces the wetting phase and results in the formation of stable residual gas structures within the porous medium. The two configurations presented in Fig. 2 correspond to the initial states prior to the downward and upward wetting-phase re-imbibition tests, respectively. Although the initial gas saturations differ slightly (approximately 0.51 and 0.58), both were prepared using identical gas injection procedures, ensuring that any observed differences in subsequent trapping behavior are attributable solely to the re-imbibition direction and not the initial gas injection process. The cylindrical volume analyzed (10.9 mm × 10.9 mm × 15.67 mm) was consistent with that used for image processing and subsequent analysis. The right panel is a magnified subregion highlighting three-phase segmentation, where gas is shown in blue, glass beads in gray, and the water phase is rendered transparent. These images depict the distribution and connectivity of gas clusters within the pore space and serve as the reference condition for evaluating the morphological evolution and stability of trapped structures under subsequent re-imbibition.

3. Results and discussion

3.1 Pore-scale evolution of residual phase morphology

The evolution of pore-scale residual gas trapping during wetting-phase re-imbibition is influenced by both capillary number and injection direction. Fig. 3 illustrates the 3D evolution of pore-scale residual gas trapping structures during wetting phase re-imbibition under varying capillary numbers and injection directions. The left panel shows downward injection aligned with gravity, while the right panel presents upward injection opposing gravity. Each row corresponds to a different $\log Ca$, ranging from -5.1 to -4.1, representing increasing injection strengths. For each condition, three consecutive re-imbibition cycles are shown, depicting the temporal evolution of residual gas distribution and bubble morphology. Under relatively low capillary number conditions ($\log \mathrm{Ca} = -5.1$), the morphology of residual gas bubbles remains stable, with limited changes observed across both injection directions. As Ca increases, more pronounced morphological alterations are observed, particularly under upward injection, where bubbles tend to fragment and redistribute more dynamically. Under downward injection, bubbles exhibit greater stability, maintaining more uniform distributions and smaller sizes throughout the cycles. In contrast, upward injection promotes bubble coalescence and migration due to buoyancy effects, resulting in larger and less stable gas clusters. These observations indicate that injection direction coupled with capillary number significantly influences the stability and spatial arrangement of trapped gas at the pore scale, with buoyancy playing a key role in destabilizing residual gas during upward injection. This effect has important implications for optimizing injection strategies in applications such as CO_2 geological sequestration and underground gas storage.

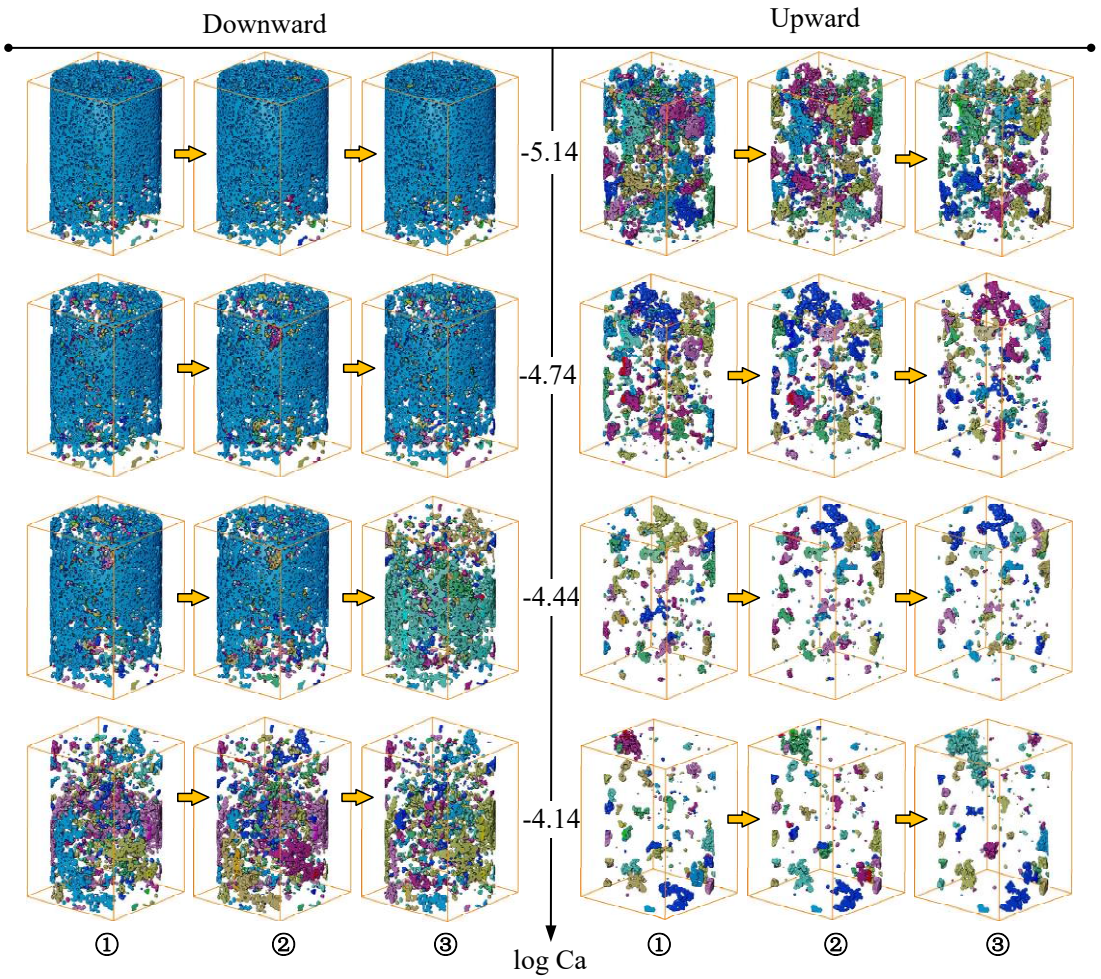

Fig. 3. Three-dimensional visualization of pore-scale residual gas trapping structures during wetting phase re-imbibition under different capillary numbers and injection directions. The left column shows downward injection aligned with gravity and the right column shows upward injection opposing gravitytle.

3.2 Residual saturation and macroscopic trapping efficiency

The residual gas saturation following each wetting-phase re-imbibition cycle at varying capillary numbers and injection directions is shown in Fig. 4. Overall, residual gas saturation decreases as Ca increases (Hu et al., 2021), but the rate of decline is significantly influenced by the injection direction. Under downward injection aligned with gravity, residual gas saturation remains relatively high even at elevated Ca, with data from three consecutive re-imbibition cycles showing limited variation, indicating stable trapping structures. In contrast upward injection opposing gravity results in markedly lower residual saturations at comparable Ca values, accompanied by greater fluctuations between cycles. This discrepancy suggests that buoyancy acts synergistically with the flow direction during upward injection, enhancing bubble detachment and mobilization, thus facilitating greater gas displacement. Conversely, during downward injection, buoyancy opposes the flow direction, generating additional trapping effects that inhibit bubble migration. When capillary forces dominate at low capillary numbers, buoyancy significantly enhances the stability of trapped gas, hindering bubble displacement. Furthermore, the multi-cycle results reveal that residual structures under downward injection are more stable, with residual saturation exhibiting minimal changes, which indicates the gradual stabilization of small bubbles and the formation of stable interconnected trapping structures. In contrast, upward injection promotes the disruption and localized coalescence of bubbles, and the migration of larger bubbles, leading to increased saturation variability. These results highlight the critical role of injection direction and flow rate in regulating gas trapping stability in subsurface storage and gas reservoir operations. To ensure long term storage security, downward injection aligned with gravity is recommended to enhance the cooperative resistance of capillary trapping and buoyancy.

As shown in Fig. 5, the relationship between residual saturation (S_r) and initial saturation (S_i) was analyzed using Land's empirical trapping model: $S_r = S_i/(1+CS_i)$. Although the initial re-imbibition cycles show noticeable deviations from the model predictions, the data progressively approach curves corresponding to a smaller dimensionless parameter C with an increasing number of cycles (Wang et al., 2023). Specifically, downward injection (aligned with gravity) is associated with

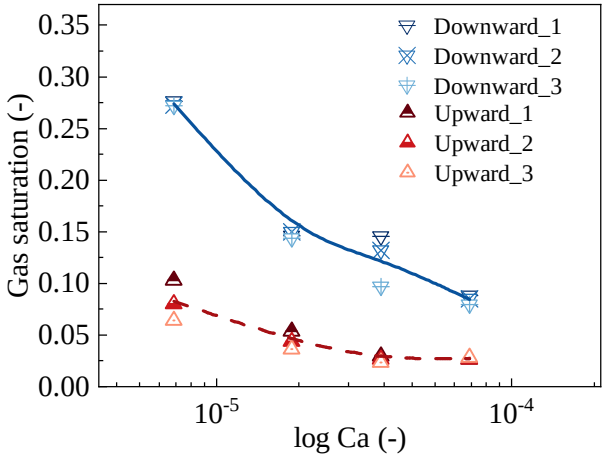

Fig. 4. Relationship between residual gas saturation and capillary number under different injection directions and successive re-imbibition cycles. Markers 1, 2 and 3 correspond to the first, second, and third re-imbibition cycles, respectively.

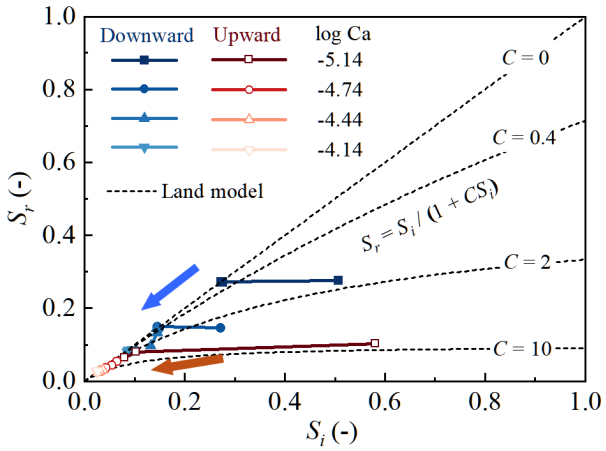

Fig. 5. Relationship between initial gas saturation (S_i) and residual gas saturation (S_r) under different injection directions and capillary numbers. The arrows illustrate the decreasing trend of residual saturation with increasing Ca.

higher residual saturations and larger C values, indicating more effective capillary trapping. In contrast, upward injection (opposing gravity) results in lower residual saturations and corresponds to lower C values, consistent with enhanced bubble mobilization due to buoyancy effects. These findings emphasize the significant influence of injection direction and capillary number on trapping efficiency, offering valuable insights for optimizing injection strategies in subsurface gas storage and CO_2 sequestration.

3.3 Morphological characteristics of residual gas bubbles

Beyond the changes in overall saturation, re-imbibition also alters the distribution of trapped gas bubble volumes, reflecting distinct pore-scale dynamics under different injection directions and capillary numbers. Fig. 6 illustrates the evolution of residual gas bubble volume distributions during multiple cycles of wetting-phase re-imbibition under varying capillary number, revealing distinct behaviors between downward (gravity-aligned, upper row) and upward (gravity-opposing, lower row) directions. Under downward injection, the distributions display a bimodal pattern. At low Ca, the distribution peaks at smaller volumes, indicating a dominance of snap-off-generated microbubbles. As Ca increases, the total bubble count rises due to fragmentation from viscous and buoyancy-induced shear, despite an overall decrease in residual saturation. In addition to the prominent bimodal structure, a secondary population of large bubbles is evident in the high-volume tail, as indicated by the circular markers, particularly at low Ca values. These stable, high-volume clusters are likely retained because buoyancy opposes the wetting-phase flow, inhibiting their upward migration and detachment. This stabilizing effect helps preserve disconnected gas structures and contributes to the broader size spectrum observed during downward injection. Conversely, upward injection exhibits a unimodal distribution, with the peak shifting toward smaller volumes and the bubble count decreasing significantly as Ca increases. This reflects enhanced bubble coalescence and mobilization, which reduces the number of trapped bubbles and promotes size homogenization. These contrasting distributions highlight how buoyancy governs bubble evolution pathways. In downward injection, buoyancy restricts bubble migration and encourages local trapping and fragmentation; in upward injection, buoyancy and flow are aligned, promoting vertical migration and inter-bubble collisions. At the pore scale, this directional alignment increases residence time and trajectory overlap, enhancing coalescence through more frequent encounters. These findings demonstrate that buoyancy influences not only macroscopic gas trapping efficiency but also the microscale morphological evolution of residual gas through direction-dependent mechanisms. This understanding is crucial for optimizing injection strategies in subsurface gas storage applications.

In addition to influencing saturation and bubble volume, re-imbibition also affects the number of residual gas bubbles, as shown in Fig. 7. Under downward injection, the bubble count increases with Ca, but the rate of increase slows at higher Ca values. Moreover, for a given Ca, increasing the number of re-imbibition cycles results in only minor fluctuations in bubble count, suggesting that the gas distribution quickly reaches a morphological equilibrium, typically within the first one to two cycles. This stabilization process is mainly driven by capillary snap-off, geometric confinement, and buoyancy opposing flow, which collectively limit bubble mobilization. Once bubbles are fragmented and occupy energetically stable pore spaces, subsequent re-imbibition fails to significantly alter the configuration. The limited vertical connectivity under downward flow further reduces the likelihood of bubble migration or coalescence, reinforcing structural persistence, consistent with the stable residual gas morphology observed at all Ca levels. In contrast, upward injection yields a decreasing trend in bubble number with increasing Ca. At low Ca, repeated re-imbibition cycles reduce the bubble count, indicating progressive coalescence or mobilization. This behavior aligns with previous observations of enhanced bubble movement and merging under buoyancy-assisted flow. Overall, the results highlight how the balance

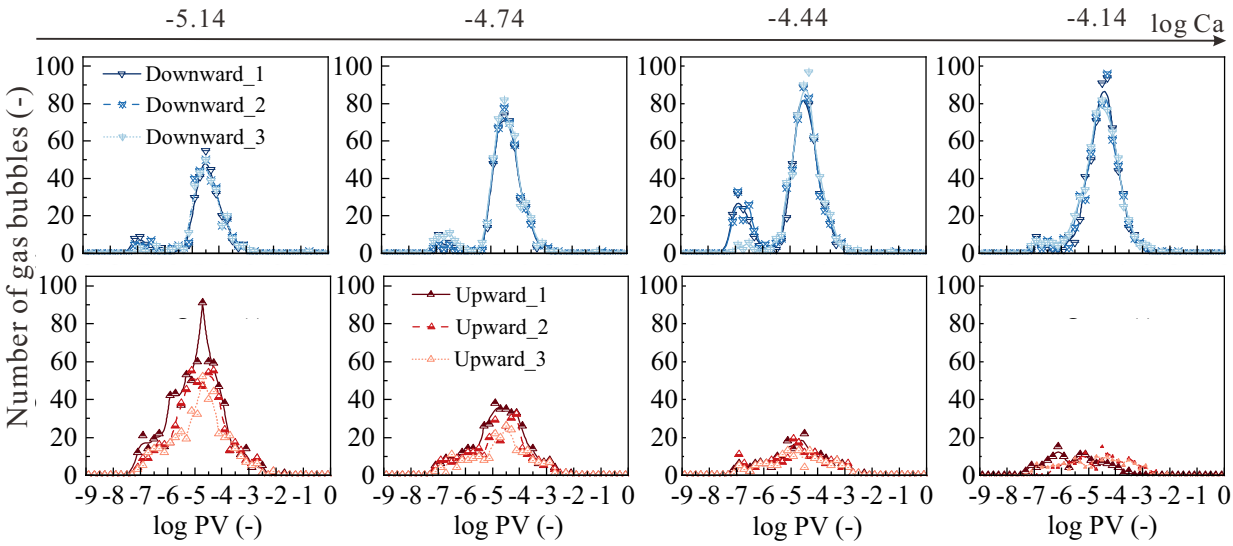

Fig. 6. Gas bubble volume distributions under varying capillary number and injection directions.

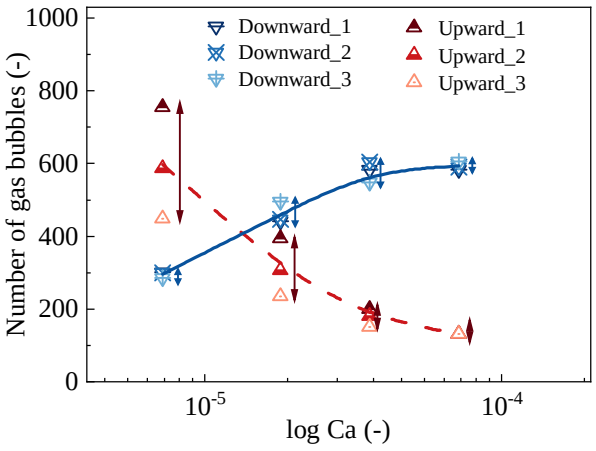

Fig. 7. Relationship between the number of residual gas bubbles and capillary number under different injection directions.

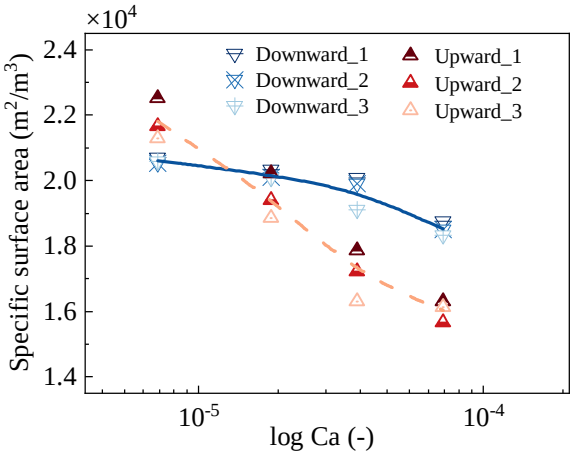

Fig. 8. Relationship between the specific surface area of trapped gas bubbles and capillary number under different injection directions and re-imbibition cycles.

of buoyancy, capillary and viscous forces regulate gas-phase morphology. Downward injections promote dense, stable distributions of small bubbles, while upward injections lead to more dynamic, less stable trapping structures.

The specific surface area of trapped gas bubbles per unit volume varies significantly with the capillary number and injection direction, as shown in Fig. 8. Under downward injection, the specific surface area decreases gradually with increasing Ca but remains relatively stable across three re-imbibition cycles. This suggests that the gas structures reach a morphological equilibrium early, consistent with the stable bubble count observed in Fig. 7. This stability results from the formation of many small bubbles evenly distributed across the pore network, which maintain a high gas-liquid interfacial area even as Ca increases. This trend also agrees with the volume distribution in Fig. 6, where higher Ca promotes fragmentation into smaller bubbles rather than their coalescence. In contrast, upward injection leads to a steeper decline in specific surface area with increasing Ca and greater variation across cycles. Buoyancy assists the flow, promoting bubble coalescence and mobilization, which reduces the number of small, trapped bubbles and favors the formation and escape of larger ones. These contrasting trends highlight the stabilizing effect of downward injection, which better preserves the gas-liquid interface area and supports both residual trapping and enhanced CO_2 dissolution under dynamic flow conditions.

3.4 Theoretical analysis of force balance on trapped bubbles

To clarify the mechanisms by which injection direction affects capillary trapping, a force balance analysis was conducted for a single gas bubble in porous media (Fig. 9). The forces considered include viscous drag from the pressure gradient, gravitational buoyancy, and capillary resistance.

According to Darcy's law, the viscous pressure gradient is:

$$\frac{\partial P}{\partial x} = -\frac{\mu u}{k} \tag{1}$$

where $\partial P/\partial x$ represents the gradient of pressure P along

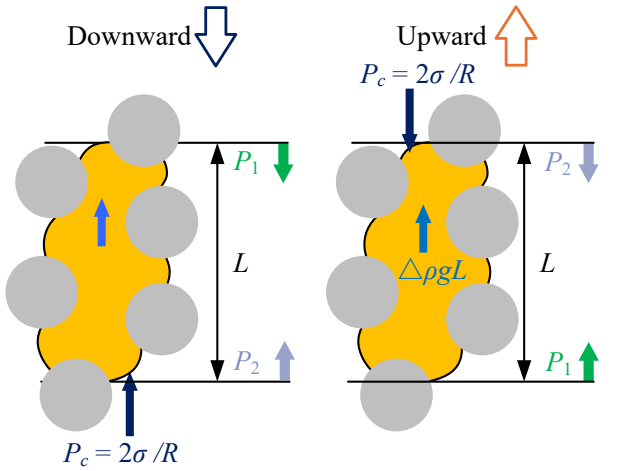

Fig. 9. Schematic illustration of the forces acting on a trapped gas bubble under downward and upward injection in a porous medium.

the x direction; k represents the permeability.

The net pressure acting on the gas bubble over a representative length L can be expressed as:

$$P_n = P_1 - P_2 - P_c - \Delta\rho gL \tag{2}$$

where P_n represents net pressure acting on the gas bubble; P_1 represents the pressure at the upstream face of the bubble (aligned with the injection flow); P_2 represents the pressure at the downstream face of the bubble; P_c represents the capillary entry pressure resisting gas movement through the pore throat ($P_c = 2\sigma/R$), R represents the radius of the pore throat at the bubble interface.

Substituting the Darcy expression yields:

$$P_d = \left(\frac{\mu u}{k} - \Delta\rho g\right) L - P_c \tag{3}$$

$$P_u = \left(\frac{\mu u}{k} + \Delta\rho g\right) L - P_c \tag{4}$$

where the subscript d and u represent the downward and upward direction, respectively. Thus, P_n can be written as:

$$P_n = \left(\frac{\mathrm{Ca}}{k} \pm \frac{\mathrm{Bo}}{d^2}\right) \sigma L - P_c \tag{5}$$

where the $\pm$ sign represents the directionality of buoyancy relative to the flow (- for downward, + for upward).

A theoretical analysis of force balance helps interpret the observed variations in residual saturation, bubble volume distribution, and specific surface area under different injection modes. In particular, the interplay between viscous, capillary and buoyant forces governs the dynamic evolution of trapped gas, and this force balance is modulated by the injection direction. As shown in Figs. 4-8, downward injection results in higher residual saturation, a greater number of small bubbles, and a higher specific surface area. This occurs because buoyancy acts against the injection flow, reducing the net driving force on gas bubbles. When the combined viscous and buoyant forces remain below the capillary entry threshold ($P_n < P_c$), bubbles are immobilized and tend to fragment under local shear, leading to stable gas trapping. In contrast, upward injections align buoyancy with the flow direction, increasing the net force acting on bubbles. When this total pressure exceeds the capillary threshold ($P_n > P_c$), bubbles are more likely to migrate, coalesce and escape from the pore structure, reducing gas retention and the interfacial area. Therefore, the theoretical force balance framework not only supports but also clarifies the directional trends observed in the experimental results, providing a mechanistic understanding of capillary trapping and offering guidance for optimizing the injection strategies in subsurface gas storage and CO_2 sequestration.

4. Conclusions

In this study, the effects of injection direction, flow rate and wetting phase re-imbibition on pore-scale gas trapping behavior in a hydrophilic porous medium have been systematically investigated using high-resolution X-ray CT imaging and quantitative morphological analysis. The results demonstrated that injection direction, coupled with buoyancy and viscous forces, plays a critical role in controlling residual gas saturation, bubble count, volume distribution, and specific surface area. Downward injection (gravity-aligned) was shown to promote bubble fragmentation, increase the proportion of small, stable bubbles, and help maintain a higher gas-liquid interfacial area even at higher capillary numbers, enhancing long-term trapping stability and potential dissolution. In contrast, upward injection (gravity-opposing) facilitates bubble coalescence and mobilization, resulting in fewer bubbles, larger residual structures, and reduced trapping efficiency. These pore-scale observations highlight the fundamental interplay between capillary, viscous and buoyancy forces in governing gas trapping mechanisms. A complementary force balance analysis further elucidated how variations in injection direction modulate the interplay between these forces acting on individual gas bubbles, offering a mechanistic insight into the distinct morphological evolutions observed in the experiments. The findings provide valuable experimental evidence supporting the optimization of injection direction and flow rate to enhance capillary trapping and storage security in CO_2 sequestration and underground gas storage operations.

5. Future work

While this study clarifies the pore-scale mechanisms of capillary trapping under varying injection directions and buoyancy conditions, several important aspects remain to be addressed by future investigations. These include the effects of wettability heterogeneity and pore structure anisotropy, which influence bubble migration, interface dynamics, and trapping efficiency. Multi-stage injections and cyclic re-imbibition schemes also warrant further research to enhance gas retention under realistic flow conditions. Specifically, repeated drainage-imbibition cycles in 3D porous media deserve more attention; although these processes have been explored in two-dimensional micromodels (Wang et al., 2023; Yang et al., 2025; Zhang et al., 2025), their behavior in 3D structures remains poorly understood. Such cycles may induce memory effects, gas redistribution, and the long-term stabilization or destabilization of gas clusters, which are critical for evaluating storage performance. Finally, applying the current framework

to different gas types (e.g., hydrogen, methane) and geological settings can help extend its relevance to broader subsurface energy storage and carbon management applications.

Acknowledgements

The authors acknowledge the support from the National Natural Science Foundation of China (No. 52206085) and the National Energy Underground Gas Storage Research and Development Center, China (No. 2024-KFKT-33). This work was also supported by JSPS KAKENHI (No. 22H03770).

Additional information: Author's email

suekane.t.aa@m.titech.ac.jp (T. Suekane).

Conflict of interest

The authors declare no competing interest.

References

Alcalde, J., Flude, S., Wilkinson, M., et al. Estimating geological CO_2 storage security to deliver on climate mitigation. Nature Communications, 2018, 9(1): 2201.

Bagheri, M., Mahani, H., Ayatollahi, S., et al. Direct pore-scale simulation of the effect of capillary number and gas compressibility on cyclic underground hydrogen storage & production in heterogeneous aquifers. Advances in Water Resources, 2023, 181: 104547.

Berg, S., Ott, H., Klapp, S. A., et al. Real-time 3D imaging of haines jumps in porous media flow. Proceedings of the National Academy of Sciences of the United States of America, 2013, 110(10): 3755-3759.

Cai, J., Jin, T., Kou, J., et al. Lucas-Washburn equation-based modeling of capillary-driven flow in porous systems. Langmuir, 2021, 37(5): 1623-1636.

Chen, Y., Clennell, B., Zhang, J., et al. Reactive transport modelling of *in-situ* CO_2 mineralization in basalt formations. Capillarity, 2024, 13(2): 37-46.

Chen, Z., Li, R., Du, Y., et al. Effect of confinement on the vapor-liquid-liquid three-phase equilibrium during CO_2 utilization and sequestration in shale reservoirs. Advances in Geo-Energy Research, 2025a, 16(3): 199-210.

Chen, X., Zhu, J., Chao, L., et al. Investigation of effect and mechanism of active water and CO_2 huff-and-puff on enhanced oil recovery in tight reservoirs. Capillarity, 2025b, 14(1): 23-34.

Hassanpouryouzband, A., Joonaki, E., Edlmann, K., et al. Offshore geological storage of hydrogen: Is this our best option to achieve net-zero? ACS Energy Letters, 2021, 6(6): 2181-2186.

He, Z., Liang, F., Meng, J. Effects of injection directions and boundary exchange times on adaptive pumping in heterogeneous porous media: Pore-scale simulation. Science of The Total Environment, 2023, 867: 161427.

He, Y., Xie, Y., Qiao, Y., et al. Estimation of underground hydrogen storage capacity in depleted gas reservoirs using CO_2 as cushion gas. Applied Energy, 2024, 375: 124093.

Herring, A. L., Andersson, L., Wildenschild, D. Enhancing residual trapping of supercritical CO_2 via cyclic injections. Geophysical Research Letters, 2016, 43(18): 9677-9685.

Holtzman, R., Dentz, M., Planet, R., et al. The origin of hysteresis and memory of two-phase flow in disordered media. Communications Physics, 2020, 3(1): 222.

Hu, Y., Patmonoaji, A., Zhang, C., et al. Experimental study on the displacement patterns and the phase diagram of immiscible fluid displacement in three-dimensional porous media. Advances in Water Resources, 2020a, 140: 103584.

Hu, Y., She, Y., Patmonoaji, A., et al. Effect of capillary number on morphological characterizations of trapped gas bubbles: Study by using micro-tomography. International Journal of Heat and Mass Transfer, 2020b, 163: 120508.

Hu, Y., Zhang, C., Patmonoaji, A., et al. Pore-scale investigation of wettability impact on residual nonaqueous phase liquid dissolution in natural porous media. Science of The Total Environment, 2021, 787: 147406.

Krevor, S., Blunt, M. J., Benson, S. M., et al. Capillary trapping for geologic carbon dioxide storage - from pore scale physics to field scale implications. International Journal of Greenhouse Gas Control, 2015, 40: 221-237.

Lenormand, R., Touboul, E., Zarcone, C. Numerical models and experiments on immiscible displacements in porous media. Journal of Fluid Mechanics, 1988, 189: 165-187.

Li, Z., Nasir, M., Wang, W., et al. Impact of oil viscosity on dispersion in the aqueous phase of an immiscible two-phase flow in porous media: An X-ray tomography study. Water Resources Research, 2023, 59(10): e2023WR034849.

Li, Y., Yang, Y., Dong, M. CO_2 capillary trapping in layered sandstone dominated by inertial force and gravity. Capillarity, 2024, 10(1): 22-28.

Lysyy, M., Ersland, G., Fernø, M. Pore-scale dynamics for underground porous media hydrogen storage. Advances in Water Resources, 2022, 163: 104167.

Maggiolo, D., Picano, F., Toschi, F. Asymmetric invasion in anisotropic porous media. Physical Review E, 2021, 104(4): 045103.

Mo, J., Zhang, C., Zheng, W., et al. Influence of binder content on gas-water two-phase flow and displacement phase diagram in the gas diffusion layer of pemfc: A pore network view. International Journal of Heat and Mass Transfer, 2024, 231: 125838.

Na, Z., Suekane, T., Hosokawa, T., et al. In-situ capillary trapping of CO_2 by co-injection. Transport in Porous Media, 2011, 90(2): 575-587.

Padhye, L. P., Srivastava, P., Jasemizad, T., et al. Contaminant containment for sustainable remediation of persistent contaminants in soil and groundwater. Journal of Hazardous Materials, 2023, 455: 131575.

Patmonoaji, A., Tahta, M. A., Tuasikal, J. A., et al. Dissolution mass transfer of trapped gases in porous media: A

correlation of sherwood, reynolds, and schmidt numbers. International Journal of Heat and Mass Transfer, 2023, 205: 123860.

Qin, X., Wang, H., Xia, Y., et al. Pore-scale investigation of water-CO2-oil flow in shale fractures for enhanced displacement efficiency and CO_2 sequestration. Engineering Geology, 2025, 348(27); 107969.

Saeibehrouzi, A., Denissenko, P., Holtzman, R., et al. Solute spreading enhancement by drainage-imbibition cycles in unsaturated porous media. Water Research, 2025, 283: 123741.

Scanziani, A., Singh, K., Menke, H., et al. Dynamics of enhanced gas trapping applied to CO_2 storage in the presence of oil using synchrotron X-ray micro tomography. Applied Energy, 2020, 259: 114136.

Spurin, C., Ellman, S., Bultreys, T., et al. The role of injection method on residual trapping at the pore-scale in continuum-scale samples. International Journal of Greenhouse Gas Control, 2024, 131: 104035.

Thaysen, E. M., Butler, I. B., Hassanpouryouzband, A., et al. Pore-scale imaging of hydrogen displacement and trapping in porous media. International Journal of Hydrogen Energy, 2023, 48(8): 3091-3106.

Wang, Z., Pereira, J.-M., Sauret, E., et al. Wettability impacts residual trapping of immiscible fluids during cyclic injection. Journal of Fluid Mechanics, 2023, 961: A19.

Wang, J., Yang, Y., Zhang, Q., et al. Pore scale modeling of wettability impact on CO_2 capillary and dissolution trapping in natural porous media. Advances in Water Resources, 2025a, 201: 104982.

Wang, S., Zhang, M., Zhang, Y., et al. Mechanisms of CO_2 huff and puff enhanced oil recovery and storage within shale nanopores. Chemical Engineering Journal, 2025b, 506: 160098.

Xue, R., Chang, Y., Wang, S., et al. Pore-scale microfluidic investigation of unsaturated CO_2 bubble morphology and interface evolution during drainage-imbibition cycles. Capillarity, 2025, 15(3): 74-86.

Yang, S., Suo, S., Gan, Y., et al. Experimental study on hysteresis during cyclic injection in hierarchical porous media. Water Resources Research, 2025, 61(3): e2024WR038923.

Zhang, R., Chen, S., Hu, S., et al. Numerical simulation and laboratory experiments of CO_2 sequestration and being as cushion gas in underground natural gas storage reservoirs. Journal of Natural Gas Science and Engineering, 2021a, 85: 103714.

Zhang, C., She, Y., Hu, Y., et al. Experimental investigation of solute transport in variably saturated porous media using X-ray computed tomography. Physics of Fluids, 2021b, 33(7): 076610.

Zhang, K., Wanyan, Q., Xu, H., et al. Dynamics of supercritical CO_2 dissolution mass transfer in porous media: Influence of cyclic injection patterns. International Journal of Heat and Mass Transfer, 2025, 252: 127442.

Zhang, C., Yuan, Z., Matsushita, S., et al. Interpreting dynamics of snap-off in a constricted capillary from the energy dissipation principle. Physics of Fluids, 2021c, 33(3): 032112.

Zhou, X., Yu, W., Lei, G., et al. Experimental study on dual benefits of improvement of CO_2 enhanced oil recovery and its storage capacity for depleted carbonate oil reservoirs. Advances in Geo-Energy Research, 2024, 12(1): 52-65.